Appl Biochem Biotechnol (2010) 162:444–459
DOI 10.1007/s12010-009-8879-2

Engineering of a *Bacillus* α-Amylase with Improved Thermostability and Calcium Independency

Marzieh Ghollasi · Khosro Khajeh · Hossein Naderi-Manesh · Atiyeh Ghasemi

Received: 7 June 2009 / Accepted: 26 November 2009 /
Published online: 23 February 2010

Abstract Successful industrial use of amylases requires that they are sufficiently stable and active at application conditions, e.g., at high temperature in starch-liquefaction process. In the present study, site-directed mutagenesis was used to enhance the thermal stability and calcium independency of a mesophilic α-amylase from *Bacillus megaterium* WHO. Mutations (A53S and H58I) were designed at the calcium-binding site based on the sequence alignment. Kinetic and thermostability parameters of the mutants were analyzed and compared with that of the wild type. In the presence of calcium, the affinity of the enzymes (wild type and mutants) toward starch was increased. In comparison to the wild type, calcium ion had more effect on the catalytic efficiency, k_{cat}/K_m, and half-life (at 60 °C) of A53S mutant. In A53S, the dependence of half-life on calcium concentration showed that the enhanced calcium binding is likely to be responsible for the increased stability. In contrast, calcium-independent mutant (H58I) possessed high thermostability. In addition, thermodynamic parameters of amylolytic reaction exhibited an increase in the activation energy and the entropy of the system. Kinetics of irreversible thermal inactivation suggests that the activation energy increased by 1.4-fold in the most stable variant.

Keywords α-Amylase · *Bacillus megaterium* · Calcium · Site-directed mutagenesis · Thermostability

Introduction

α-Amylases (1,4-α-D-glucan glucanohydrolase; EC 3.2.1.1) are enzymes that catalyze the hydrolysis of the internal α-1,4-glucosidic linkage in starch and related oligosaccharides [1]. Enzyme produced by *Bacillus* has been studied for several important industrial applications

M. Ghollasi · K. Khajeh (✉) · H. Naderi-Manesh
Department of Biochemistry and Biophysics, Faculty of Biological Science, Tarbiat Modares University, P.O Box: 14115-175, Tehran, Iran
e-mail: khajeh@modares.ac.ir

A. Ghasemi
Institute of Biochemistry and Biophysics, University of Tehran, P.O. Box: 13145-1384, Tehran, Iran

such as sugar, brewing, food, and detergents [2]. Because of their high thermostability, the *Bacillus* α-amylases have found widespread use in industrial processes, and much attention has been devoted to optimizing these enzymes for the very harsh conditions [3]. A characteristic feature of α-amylases is their requirement of calcium ions for activity and structural stability [4]. All known α-amylases contain at least a single calcium ion per molecule, but one or more additional calcium-binding sites have been identified depending on the origin of α-amylase [5].

Protein engineering has already been used to enhance enzyme thermostability, but it is usually not clear which amino acid substitutions should be made particular in cases that the structural information for the protein is not available [6]. It is reasonable that, by comparing the primary sequences of thermophilic enzymes and mesophilic counterparts, the non-conserved regions, as those possibly linked to the thermostable phenotype, can be identified. Most effective regions for substitution will be the more flexible for being the more labile [7].

α-Amylase from *Bacillus megaterium* WHO (BMW), isolated from hot springs of Ramsar (the north of Iran), was used in this research in order to assess the role of residues near the hypothetical Ca-binding site in thermal stability and their potential use as the targets for site-directed mutagenesis in modifying enzyme function. WHO represented a strain of genus *B. megaterium* according to a phylogenetic analysis of the 16S rDNA and is highly radio resistant [8]. Following preliminary characterization, a series of mutations was introduced in BMW-amylase having 98% sequence identity to *B. megaterium* with the aim of increasing stability and calcium independency. Sequence alignment of BMW-amylase with other α-amylase family enzymes demonstrated 50% sequence identity and 67% sequence similarity with *Halothermothrix orenii* α-amylase (AmyA). *H. orenii* is a thermohalophilic bacterium that produces two kinds of α-amylases named AmyA and AmyB, showing only 23% identity with other amylases isolated from the same bacterium [9, 10]. Crystal structure of AmyA shows that two calcium-binding loops are located in domain A [11]. In the fragment of domain A where the calcium-binding site is located, identity and similarity rise to 63% and 81%, respectively. In regard to high sequence identity between BMW-amylase and AmyA, we chose AmyA as a model for identifying the best positions for site-directed mutagenesis in order to improve the thermostability. Amino acid substitutions in Ca-binding site far from the active site were carried out to improve thermostability while avoiding structural disruption. Here, the effects of the calcium ion on the thermal inactivation of BMW-amylase and its variants were investigated. Kinetic and thermodynamic parameters were also studied.

Materials and Methods

Chemicals

The following chemicals were purchased from commercial sources: starch, dinitrosalicylic acid (DNS) (Sigma Chemical Co., St. Louis, Mo, USA); $MgCl_2$, dNTP, and Taq polymerase (Fermentas, Vilnius, Lithuania); restriction enzymes (Boehringer Mannheim); Ni-nitrilotriacetic acid (NTA) column (Qiagen, Munich, Germany); Tris (liofilchem, Italy); $CaCl_2$ (Merck, Germany). All other chemicals were of analytical grade.

Bacterial Strains and Plasmids

B. megaterium WHO was used as a source of genomic DNA. *Escherichia coli* XL1-blue and *E. coli* BL-21 were used as the hosts for cloning and expression experiments. Plasmid pET-21a served as the vector for construction of expression vector.

Media

B. megaterium WHO was grown aerobically on solid plates containing agar (8 g/L), nutrient agar (28 g/L), and yeast extract (5 g/L) at 30 °C. *E. coli* was routinely grown at 37 °C in Luria–Bertani (LB) medium [12] supplemented with ampicillin (100 mg/mL) or isopropyl-β-D-thiogalactopyranoside (IPTG,1 mM) or 5-bromo-4-chloro-3-indolyl-β-D-galactopyranoside (X-Gal; 40 μg/mL) if required.

DNA Isolation and Manipulation

Genomic DNA was isolated from *B. megaterium* WHO by phenol-chloroform method [13]. Plasmid isolation from *E. coli* was performed by the plasmid extraction miniprep kit (Bioneer, Korea). Manipulating of DNA molecules was performed according to Sambrook and Russell [12].

Cloning of BMW-Amylase

Polymerase chain reaction (PCR) amplification was carried out using Taq polymerase at the following temperature profile: 94 °C for 4 min followed by 35 cycles of 94 °C for 45 s, 50 °C for 1 min, and 72 °C for 1.5 min. The specific primers were designed according to the similarity observed through alignment of α-amylase genes from *B. megaterium*.

5′ATGAAAGGGAAAAAATGGACAG3′ and 5′TTATTTTATTAAAACCGTCCGATTC 3′ were used as forward and reverse primers, respectively. The PCR product was cloned into pTZ57R/T plasmid using T/A Ins clone kit (Fermentas, Vilnius, Lithuania). Nucleotide sequencing of the α-amylase gene was performed using an automatic sequencer (Millgen, France). Homology searches were carried out using BLAST through the National Center for Biotechnology Information (NCBI) server. The nucleotide sequence data were submitted to the GenBank under the accession number of ABU54057.

Plasmid pET-21a containing the IPTG-inducible T_7 promoter (Novagen) was used for expression in *E. coli*. The cloning primers were designed containing the restriction sites for NdeI and Hind III. PCR amplification was performed using PWO polymerase (Boehringer Mannheim) and pTZ57R/T vector containing α-amylase gene as the template at the following temperature profile: 94 °C for 4 min and 35 cycles of 94 °C for 45 s, 66.5 °C for 1 min, and 72 °C for 1.5 min. The PCR product was subcloned in the pET-21a plasmid. The ligation reaction was done using T_4-DNA ligase (Fermentas) at 16 °C for 12 h. The ligation mixture was used for transformation of *E. coli* XL1-blue, and the clones containing recombinant plasmid (pAmyWS) were placed on solid plates containing agar (1.5% (*w*/*v*)), yeast extract (5 g/L), tryptone (10 g/L), NaCl (10 g/L), and ampicillin (100 mg/mL). Amylase activity could be seen after overnight growth of the positive clones on LB medium containing ampicillin at 37 °C. Sequencing confirmed the correct insertion of the gene.

Subcloning and Expression of the Open Reading Frame Encoding α-Amylase without Signal Sequence in *E. coli*

Primers were designed for the amplification of the open reading frame (ORF) encoding α-amylase without signal sequence in pAmyWS. The primer sequences used were as follow:

Primer A: 5′ GGAATTCCATATGGTACATAAAGGTAAGTCTGAAGC 3′
Primer B: 5′ CCCAAGCTTCTTTATTAAAACCGTCCGATTC3′

PCR was performed in a thermocycler using 20 pmol of each primer plus pAmyWS as a template. The reaction conditions were as follows: 94 °C for 5 min and 30 cycles of 94 °C for 1 min, 55 °C for 45 s, and 72 °C for 1 min. The reaction mixture contained 10 μM dNTp, 25 mM KCl, 5 mM $(NH4)_2SO_4$, 2 mM $MgSO_4$, 2.5 U of PWO polymerase in a reaction volume of 25 μL. Products of PCR were purified with a cleanup kit (Bioneer, Korea) and were used for subcloning in pET-21a. Obtained recombinant plasmid (pAmyW) was used for sequencing and mutagenesis. Sequencing was performed using an automated DNA sequencer (Millgen, France). Both strands of the DNA were sequenced and the complete sequence obtained using BLAST program by NCBI server.

Site-Directed Mutagenesis

Mutagenesis was carried out using quick-change method described by Fisher and colleagues [14]. Chemically synthesized oligonucleotides (35–40 mers) were used (Bioneer, Korea). Based on quick-change site-directed mutagenesis method, two pairs of primers were designed as follows:

A53S primer F: 5′GTAAACTCTTTTTACGATAGCAATAAAGATGGACATGGTG 3′
A53S primer R: 5′ CACCATGTCCATCTTTATTGCTATCGTAAAAAGAGTTTAC3′
H58I primer F: 5′ GATGCAAATAAAGATGGAATTGGTGATTTAAAAGGTCTGAC3′
H58I primer R: 5′GTCAGACCTTTTAAATCACCAATTCCATCTTTATTTGCATC 3′

The PCR reaction mixture contained 0.2 μg template DNA, 10× PCR buffer, 0.2 mM of each dNTp, 15 μM of each primer, and PWO polymerase (1.25 U) in 50 μL. The mixture was heated at 95 °C for 5 min and then subjected to thermal cycling (22 cycles of 94 °C for 1 min, 55 °C for 1 min, and 68 °C for 13 min). The PCR product was incubated in a digestion reaction with DpnI at 37 °C for 12 h. The digestion reaction transformed to *E. coli* XL1-blue by chemical method [12] for each mutation. Five clones were selected randomly for sequencing, and the mutagenesis was confirmed. *E. coli* BL-21, harboring a recombinant plasmid, was grown overnight at 37 °C in 25 mL broth containing ampicillin (100 mg/mL). An overnight culture was inoculated into 1 L fresh broth (1% inoculation) containing ampicillin (100 mg/mL); incubation at 37 °C was continued until an optical density at 600 nm reached 0.5–0.7. The inducer isopropyl-β-D-thiogalactopyranoside was added (final concentration, 1 mM) and incubated for another 6 h at 25 °C. Cells were harvested by centrifugation at 8,000×*g* for 20 min at 4 °C, and the cell pellet was resuspended in the lysis buffer containing NaCl, 1 M; Tris, 50 mM; imidazole, 2 mM; phenylmethylsulfonyl fluoride,1 mM; glycerol 10% (*v*/*v*), pH 8.0. The cells were disrupted by sonication and then centrifuged at 15,000×*g* for 30 min at 4 °C. The supernatant, used as the crude extract, was applied to Ni-NTA column equilibrated with lysis buffer (pH 8.0). The column was washed with a linear gradient of washing buffer (NaCl, 1 M; Tris, 50 mM; imidazole, 30, 40, or 60 mM, pH 8.0) and eluted with buffer containing the same components of washing buffer except 250 mM imidazole. The eluted fractions containing amylase activity were pooled and dialyzed twice against 20 mM Tris–HCl buffer (pH 7.2). The solution was then used for determination of protein concentration based on Bradford procedure [15] and thermostability experiments. Sodium dodecyl sulfate polyacrylamide gel electrophoresis (SDS-PAGE) was carried out by the method of Laemmli [16]. A high-molecular-weight marker (Fermentas) was used, and protein bands were detected by staining with Coomassie Brilliant Blue R-250.

Circular Dichroism and Fluorescence Spectroscopy

Circular dichroism measurements were conducted on an AVIV model 215(USA) spectropolarimeter equipped with a thermostatically controlled cell holder. Results were expressed as molar ellipticity [θ] (° cm^2 $dmol^{-1}$), based on a mean amino acid residue weight (MRW) assuming average weight of 54,450 g/mol for BMW-amylase. The molar ellipticity [θ] was calculated from the formula $[\theta]\lambda = (\theta \times 100\,\mathrm{MRW})/(cl)$, where c is the protein concentration in milligrams per milliliter, l the light path length in centimeters, and θ the measured ellipticity in degrees at wavelength λ. Each spectrum is an average of at least two scans. All spectra were background-corrected, smoothed, and transformed into mean residue ellipticity [θ]. Fluorescence studies were carried out on VARIAN luminescence spectrometer CARY Eclipse. Intrinsic fluorescence was determined using 0.02 mg/mL protein and an excitation wavelength of 280 nm. Emission spectra were recorded between 300 and 400 nm.

Enzyme Activity and Biochemical Characterization

α-Amylase activity was determined by measuring the amount of reducing sugars released during incubation with starch. Eighty microliters of 1% (*w*/*v*) starch was dissolved in 20 mM Tris–HCl buffer (pH 7.2); 20 μL of enzyme solution was added, and the samples were incubated at 30 °C for 30 min. The reaction was stopped by adding DNS reagent, and the amount of reducing sugars released was determined by dinitrosalicylic acid method [17]. One unit of amylase activity is defined as the amount of enzyme that releases 1 μmol of reducing sugars (with maltose as the standard) per minute under the assay conditions specified. To determine the influence of temperature on the enzymatic activity, samples were incubated at temperatures from 20 to 100 °C for 5 min using thermoblock or water bath, and the enzyme activity was measured by DNS method.

Thermal Inactivation

Thermal stability was determined at five temperatures (50, 55, 60, 65, and 70 °C) in 20 mM Tris–HCl buffer (pH 7.2) using 0.06 mg/mL enzyme. At various time intervals, 20 μL aliquots were removed and diluted into 100 μL of an assay solution (80 μL starch 1% (*w*/*v*), 2 or 5 mM $CaCl_2$) for the measurement of residual activity at 30 °C for 30 min. Plots of the log of residual activity versus time were linear, indicating a first-order decay process under these conditions. T_{50} is the temperature of incubation at which 50% of the initial amylase activity is lost during 30 min incubation.

Enzyme Kinetics

In order to determine kinetic parameter, measurements were carried out using 15 different substrate concentrations, and the final concentration of the enzyme was 0.06 mg/mL. We have blanks for each starch concentration, and the differential absorbance was used to determine the activity. Steady-state kinetic parameters K_m, V_{max}, k_{cat}, and k_{cat}/K_m for BMW-amylase and its variants were determined by a fit of initial velocities to the Michaelis–Menten equation. The results are mean value of three independent experiments, and they were repeated for reproducibility.

Calculation of Thermodynamic Parameters

The rate constants of amylolytic reaction (k_{cat}) and inactivation (k_{inact}) were used to calculate the activation energy according to the Arrhenius equation [18].

$$k = Ae^{-E_a/RT}$$

Where k (s^{-1}) is the rate constant at temperature T (K), A is a pre-exponential factor related to steric effects and the molecular collision frequency, R is the gas constant (8.314 J $mol^{-1} K^{-1}$), and E_a the activation energy of the reaction. Hence, a plot of ln k as a function of $1/T$ gives a curve of slope $-E_a/R$. The thermodynamic parameters of activation were determined as follows:

$$\Delta G^{\#} = RT\ln(k_B T/h) - RT\ln k_{cat}$$

$$\Delta H^{\#} = E_a - RT$$

$$\Delta S^{\#} = \left(\Delta H^{\#} - \Delta G^{\#}\right)/T$$

Where k_B is the Boltzmann constant (1.3805×10^{-23} J K^{-1}), h the Planck's constant (6.6256×10^{-34} J s), and k (s^{-1}) is the rate constant at temperature T (K).

All results are the mean from at least three repeated experiments in a typical run to confirm reproducibility.

Results and Discussion

Cloning and Sequencing of the Amylase Gene

Based on the high homology of *B. megaterium* WHO 16S rDNA and *B. megaterium*, two primers were designed for two ends of α-amylase gene of *B. megaterium* in GenBank. Using chromosomal DNA as the template, the single band of PCR product was isolated and ligated with pTZ57R/T plasmid. The ligation mixture was used to transform *E. coli* XL1-blue. One of the purified plasmids was used for sequencing. The entire insert (1,583 bp) in pTZ57R/T plasmid was sequenced in both directions, and one ORF that encodes α-amylase was identified based on sequence homology. This gene is referred to as amyWS with the length of 1,563 bp that encodes a protein of 520 amino acids with a predicted molecular mass of 57 kDa. The G+C content of amyWS is 40.37%. Using a method that incorporates a prediction of cleavage sites based on a combination of several artificial neural networks and hidden Markov models [19], a signal sequence of 25 amino acids was determined. The cleavage site was located between Ala^{25} and Glu^{26}, resulting in a protein with a predicted mass of 54.4 kDa. The 25 residues upstream of the N terminal (MKGKKWTALALTLPLAASLSTGVHA) showed all of the characteristics of a prokaryotic signal peptide (Fig. 1). With respect to the Sec-type signal peptide, the N-region containing two or three arginine (R) or lysine (K) residues determines the orientation of the signal peptide in the membrane due to its relatively high positive charge. Helix-breaking proline (P) or glycine (G) residues are often found in the middle of

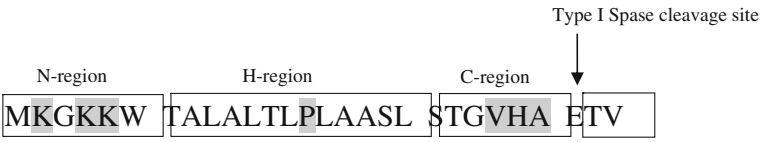

Fig. 1 The signal peptides have a tripartite structure: a positively charged N-domain (N), a hydrophobic H-domain (H) and a C-domain (C) containing specific cleavage site. The three lysine (*K*) residues in the N-region, helix-breaking proline (*P*) residue in the middle of the H-region and the C-region with the consensus sequence Val–X–Ala at positions −1 and −3 relative to the cleavage site are *shaded gray*

H-region that is believed to adapt an α-helical conformation in the membrane. The C-region commonly carries a type-I Spase (signal peptidase) cleavage site, with the consensus sequence Ala–X–Ala or Val–X–Ala at position −1 and −3 relative to the cleavage site [20]. By using BLAST to screen the GenBank and Swiss-Prot databases, only three proteins having a significant similarity score were identified (*B. megaterium*, *Bacillus Wcs10*, and *Bacillus Ws06* α-amylases). *B. megaterium* amylase showed 99% similarity and 98% identity with BMW-amylase. Among the results obtained from the BLAST, only AmyA from *H. orenii* had been structurally determined by previous studies; therefore, we used AmyA as a model for prediction of calcium-binding sites and determination of suitable regions for thermostabilization in this research. The enzyme neither has any cysteine residue nor disulfide bridge, the most sensitive protein structural elements of destruction at high temperatures [21]. Four consensus sequence characteristic of all α-amylase family enzymes [22] were present in AmyWS. Enzymatic polysaccharide hydrolysis typically involves a catalytic triad composed of acidic residues that are Asp 233, Glu 272, and Asp 339 in BMW-amylase.

Expression and Purification of α-Amylase in *E. coli* BL-21

The amyWS gene with the signal sequence and ATG start codon was subcloned into expression vector pET-21a under control of T_7 promoter. After induction with IPTG and lactose (1 and 4 mM as the final concentrations, respectively), supernatant of sonicated cells were collected from 1 L culture and applied to Ni-NTA column for purification. The purified protein revealed one band with apparent mass of 57 kDa on SDS-PAGE (Fig. 2). The obtained protein band was weak, and the recombinant protein was detected in the cell debris. In the presence of different concentrations of IPTG and lactose, the same amount of soluble enzyme was achieved. In order to increase the amount of enzyme, the α-amylase gene was subcloned into pET-21a without predicted signal sequence. This plasmid was named as pAmyW. Best results were gained when α-amylase was expressed in pAmyW, showing that targeting of the protein to the cell membrane diminishes as a result of omitting signal sequence in the α-amylase gene. Consequently, the most amount of enzyme in the soluble fraction was gained. Staining Coomassie Brilliant Blue revealed a single homogenous band in all cases (Fig. 2).

Mutation Selection in BMW-Amylase

As mentioned earlier, the only α-amylase with known structure and closest sequence homology with BMW-amylase was AmyA from a true halo-thermophilic bacterium *H. orenii*. AmyA is active in a broad range of salt concentration, and its optimal temperature is above 65 °C [11]. The crystal structure of *H. orenii* α-amylase showed three distinct domains, A, B, and C. Two calcium-binding loops are located in domain A. AmyA

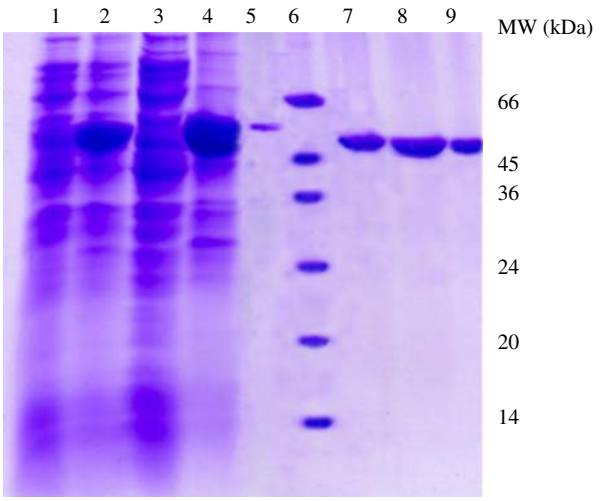

Fig. 2 SDS-PAGE analysis of recombinant BMW-amylases. *Lane 1* total proteins before induction; *lane 2* total protein after induction; *lane 3* supernatant of sonicated cells; *lane 4* pellet of sonicated cells; *lane 5* purified α-amylase with signal sequence; *lane 6* molecular-weight marker (14, 20, 24, 36, 45, 66 kDa); *lane 7* purified wild-type α-amylase without signal sequence; *lane 8* purified mutant α-amylase (A53S); *lane 9* purified mutant α-amylase (H58I)

showed the involvement of Asp^{44}, Asp^{46}, Asp^{48}, Ile^{50}, and Asp^{52} in the first calcium-binding loop (their counterpart residues in BMW-amylase are Asp^{52}, Asn^{54}, Asp^{56}, His^{58}, and Asp^{60}) and Asp^{65}, Asp^{67}, Thr^{70}, and Asp^{73} in the second calcium-binding loop. In regard to the role of calcium ion in thermal stability of amylases by using blastp program, we identified some different amino acids in the first Ca-binding site of *H. orenii* compared to BMW-amylase (e.g., substitution of His^{58} in BMW-amylase with Ile^{50} in AmyA). Besides the calcium-binding site residues, there are also some differences in the loop such as replacement of Ala^{53} in BMW-amylase with Ser^{45} in AmyA (Fig. 3). The two mutations, A53S and H58I, were chosen based on the reasons mentioned above.

Expression, Purification, and Biochemical Characterization of Wild-Type and Mutated α-Amylases in E. coli BL-21

The plasmids containing mutated α-amylase gene were transformed to *E. coli* BL-21. Expression and purification of the mutated enzyme was carried out using the same procedure as the wild type. SDS-PAGE and gel staining revealed the single band of protein (Fig. 2). Circular dichroism (CD) was used to investigate the changes of secondary

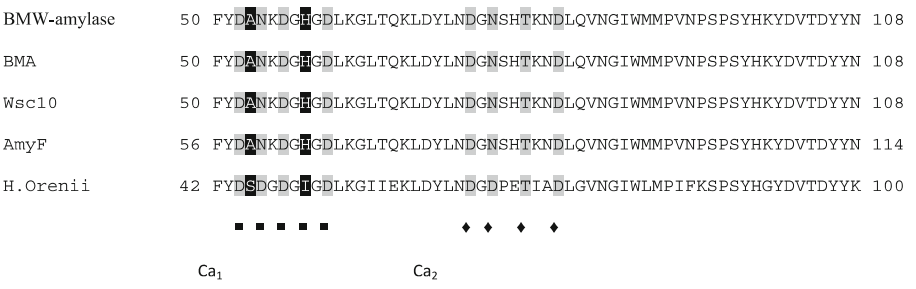

Fig. 3 Multiple alignments of N-terminal sequence of BMW-amylase and related protein in the GenBank and Swiss-Prot databases. The amino acids involved in calcium binding were designed by the *closed squares* and *closed diamonds* for the first and second calcium-binding sites, respectively. Amino acid residues selected for SDM (site-directed mutagenesis) are shaded black

structures in different variants. Figure 4a illustrates the CD spectrum of wild type and mutants. The profile of wild type is essentially identical to that of the variants, indicating that the mutations did not result in significant changes in the secondary structure content. The spectrum is typical of an α-helical protein with a large negative ellipticity at 222 nm. As shown in Fig. 4b, the intrinsic fluorescence spectrum obtained by fluorescence emission from Trp residues near 340 nm was identical for all enzyme variants. Far UV CD spectra indicated that the overall secondary structure was not substantially altered. Determination of

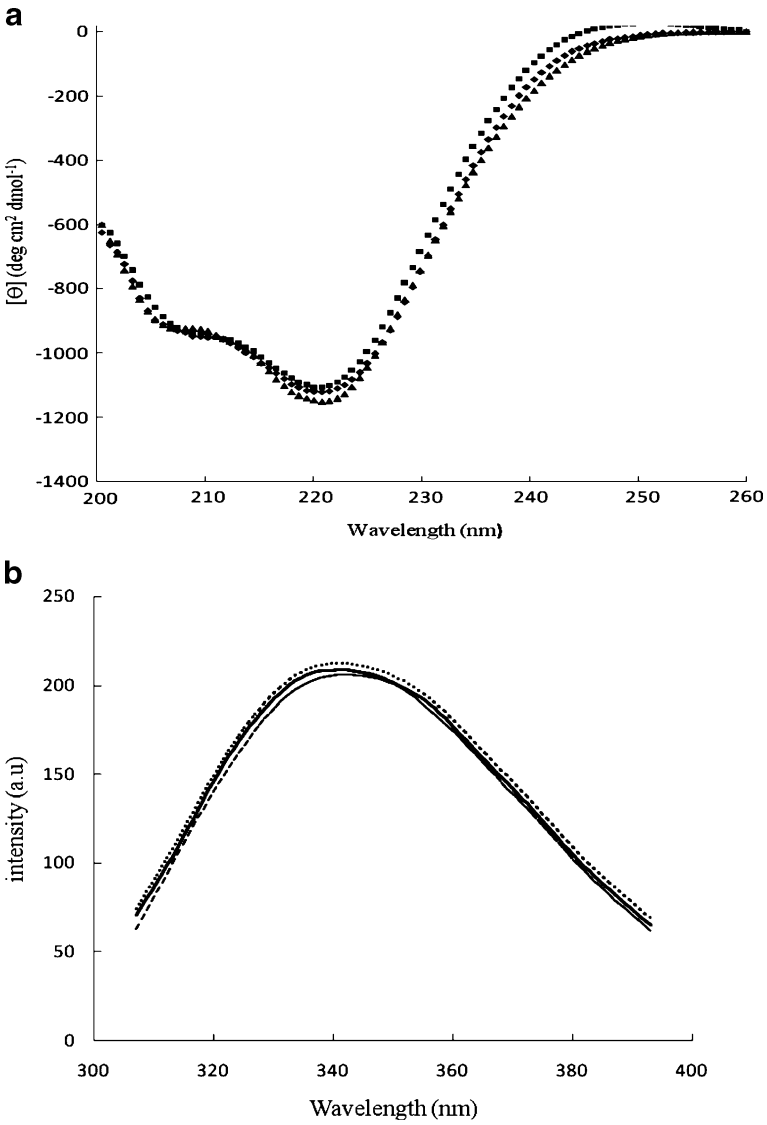

Fig. 4 Secondary structure analysis of wild-type (*closed squares*, *solid line*), A53S (*closed diamonds*, *dotted line*) and H58I (*closed triangles*, *dashed line*) variants as measured by CD (**a**) and fluorescence (**b**). CD and fluorescence spectra were recorded at 25 °C with 0.2 and 0.02 mg/mL enzyme concentrations in Tris buffer (pH 7.2), respectively

temperature profile showed that the optimum temperature for wild type, A53S, and H58I was approximately 60, 65, and 60 °C, respectively (Table 1). Also, the presence of calcium ion in different concentrations did not have noticeable effect on optimum temperature (Fig. 5).

Kinetic and Activation Parameters

The kinetic parameters (K_m and V_{max}) of the wild type and mutants were measured in two concentrations of $CaCl_2$ at 30 °C, with starch as the substrate (Table 1). It is significant that the kinetic parameters of wild type and mutants revealed a clear trend to decrease both k_{cat} and K_m in presence of $CaCl_2$. As it will be shown in the next section, thermal stability of the mutant was enhanced in comparison to the wild type. Increase in thermal stability of engineered enzymes has often been reported to be accompanied with a decrease in their catalytic activity at moderate temperature, presumably as a consequence of the overall protein rigidity [23, 24]. A higher affinity of the enzyme toward substrate in the presence of $CaCl_2$ could be for an improved electrostatic potential of the protein surface for substrate binding at the active site [25]. On the other hand, a single amino acid substitution as in A53S and H58I results in an increased K_m compared to the wild-type enzyme. Although the overall activity (k_{cat}/K_m) has not improved, about 80% of activity has been maintained in the case of A53S mutant and in presence of 5 mM Ca^{2+}. Specific activities of enzymes were recorded between 25 and 80 °C in order to construct Arrhenius plots (data not shown). The H58I mutant exhibited thermodynamic activation parameters different from the others (Table 1): higher $\Delta H^{\#}$ values reflecting the increased thermodependence and higher $\Delta S^{\#}$ possibly reflecting increased conformational change between the ground-state ES (enzyme-substrate) complex and the activated transition state [25].

Thermostability of Wild-Type and Mutated BMW-Amylase

Thermostability as Measured by Rate of Inactivation

The method that has been used to analyze the heat inactivation rate constants of α-amylases requires enzyme incubation at high temperatures and cooling in ice before measurement of the residual activity [25]. Thermostability of the wild-type and mutant enzymes (A53S and H58I) was examined at five different temperatures (50, 55, 60, 65, and 70 °C). For examining the effect of calcium on enzyme thermostability, two concentrations of Ca^{2+} (2 and 5 mM) were used. As shown in Fig. 6a–c, calcium ion has a considerable effect on thermostability of wild type and A53S mutant at 60 °C. Similar results have been obtained at other temperatures (data not shown). In the absence of $CaCl_2$, the H58I mutant was much more stable than the wild type and A53S; there was a sevenfold increase in the residual activity of H58I mutant after 30 min of incubation as compared to the wild type. An Arrhenius plot (ln residual activity versus $1/T$) for amylolytic reaction was made covering the temperature range of 50–70 °C. It is clear that the thermostability of the wild type and A53S mutant is calcium dependent at different temperatures, whereas H58I thermostability is less calcium dependent (Fig. 7–c). Increasing Ca^{2+} concentration up to 10 mM had no effect on the half-life ($t_{1/2}$) of H58I mutant at 60 °C. While in the presence of 2 mM $CaCl_2$ at 60 °C, the percentage of residual activity in both the wild type and A53S changed after 30 min of incubation, no change was observed in H58I.

Calcium is essential for maintenance of the structural integrity of α-amylase, and removal of this divalent cation leads to decreased thermostability and/or decreased

Table 1 The kinetic constants of WT and mutants in the absence and presence of 2 and 5 mM $CaCl_2$.

Enzyme	$[Ca^{2+}]$ (mM)	Kinetic parameters						Activation				Inactivation			
		$K_{m(mg/mL)}$	$k_{cat(s^{-1})}$	k_{cat}/K_m (s^{-1} mg^{-1} mL)	T_{opt} (°C)	T_{50} (°C)	$t_{1/2(min)}$	E_a (kcal /mol)	$\Delta H^{\#}$ (kcal /mol)	$\Delta G^{\#}$ (kcal /mol)	$\Delta S^{\#}$ (cal /molK)	E_a (kcal /mol)	$\Delta H^{\#}$ (kcal /mol)	$\Delta G^{\#}$ (kcal /mol)	$\Delta S^{\#}$ (cal /molK)
WT	0	2	25.7	12.5	60	52.9	7	9.5	8.9	12.6	-12.2	37.4	36.7	21.1	47
	2	1.4	19.9	13.8	60.3	55	12.6	9.9	9.3	12.6	-10.9	46.9	46.3	21.5	74.5
	5	1.4	19.9	13.8	60.7	57	17.3	10.2	9.6	12.6	-9.9	53.9	53.2	21.7	94.8
	0	1.7	22.4	13.3	65	56.6	14.4	9.8	9.2	12.6	-11.2	54.4	53.7	21.6	96.5
A53S	2	1	15.3	15.3	65.4	64.3	69.3	10.4	9.8	12.6	-9	65.1	64.4	22.6	125.5
	5	0.54	9.8	18	65.5	64.5	86.6	10.8	10.2	12.5	-7.7	74.8	74.2	22.7	154.4
	0	2.2	27.4	12.3	60.1	60	30.1	11.2	10.6	12.5	-6.5	62.1	61.4	22	118.3
H581	2	1.6	22.6	13.8	60.5	60	33	12	11.4	12.5	-3.6	66.4	65.7	22.1	130.9
	5	1.5	20.7	13.6	60.8	60	34.6	12	11.4	12.5	-3.6	65.7	65	22.1	128.8

T_{opt} and T_{50} of thermoinactivations were obtained in different $[Ca^{2+}]$. Thermodynamic parameters for amylolytic reaction were determined at 30 °C, and thermodynamic parameters for irreversible thermoinactivation ($k=k_{inactivation}$) were determined at 60 °C

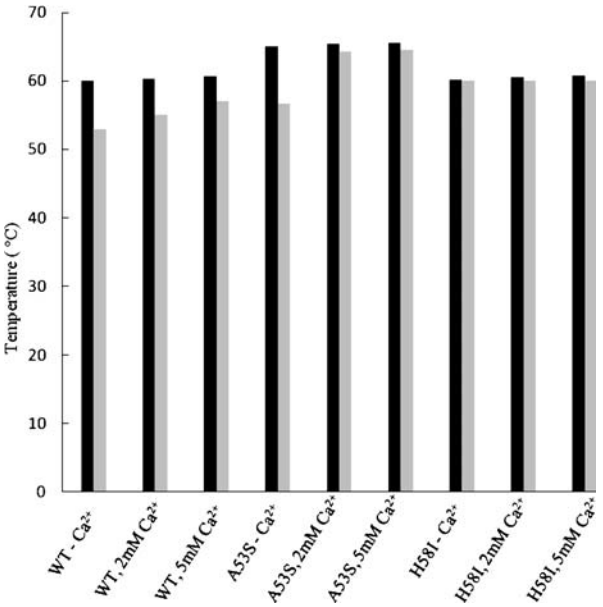

Fig. 5 Relationship between T_{opt} (*black columns*) and T_{50} (*gray columns*) for the wild type and its variants in different calcium concentrations

enzymatic activity [26]. This fact was confirmed by significant reducing of inactivation rate after addition of calcium ion. This report is providing proof that calcium actually contributes to improve the structural integrity of BMW-amylase. Our preliminary data indicated that in AmyA, calcium precisely locates around a loop containing charged residues, and the calcium binding is affected by electrostatic forces. In the case of Ala 53 Ser mutant, it appears that introducing an amino acid with electron-donating group can increase the electrostatic interactions so that the $CaCl_2$ dependency and thermostability of the mutant will be increased. The His 58 Ile mutant represents a BMW-amylase variant whose stability is largely independent of calcium concentrations and, at lower calcium concentrations, is considerably more stable than the wild-type enzyme. It could be suggested that His has no interaction with $CaCl_2$ so that its thermostability is not affected by $CaCl_2$ concentration. It is assumed that the aliphatic side chain of Ile can increased the number of hydrophobic contacts and so the increased thermostability of protein.

Thermostability as Measured by Calcium Dependency

To probe the Ca-binding properties further, affinity of enzymes to Ca^{2+} was identified by measurements of the half-lives of wild type and its variants at 60 °C as a function of $CaCl_2$ concentration (Fig. 8). Supposing that the shift in the curve reflects a change in Ca^{2+} affinity, we found that wild type is calcium dependent to some extent; A53S is highly calcium dependent, and H58I is calcium independent. The continuing need for novel α-amylases that do not require Ca^{2+} has been emphasized. There are few α-amylases obtained from *Bacillus* sp. with Ca-independency properties of thermal stability [27]. The occurrence of calcium-independent amylases was also reported in *Bacillus circulans* [28], *Bacillus acidocaldarius* [29], *Bacillus brevis* [30] and *Bacillus thermooleovorans* NP54. Furthermore, the thermostability of a calcium-free α-amylase from an alkalophilic *Bacillus* sp. has been improved by protein engineering [31].

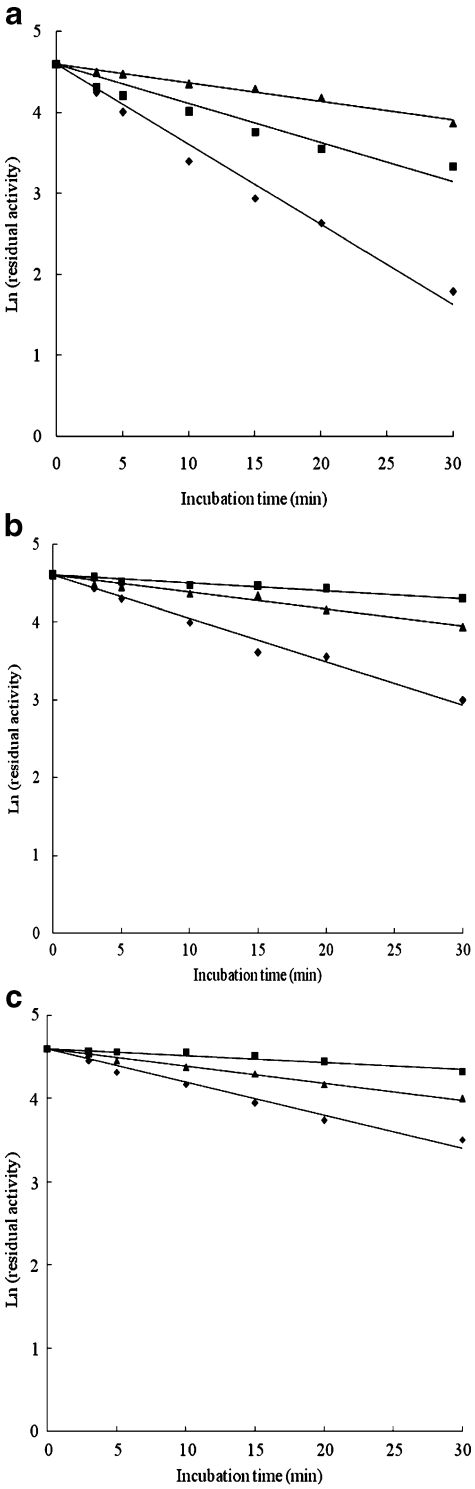

Fig. 6 First-order thermal inactivation of BMW-amylase variants at 60 °C in 0 Mm (**a**), 2 mM (**b**), and 5 mM $CaCl_2$ (**c**). The enzymes, wild-type (*closed diamonds*), A53S (*closed squares*), and H58I (*closed triangles*), were prepared in 20 mM Tris–HCl buffer (pH 7.2), and the remaining activity was measured. For more details, please see "Materials and Methods" section

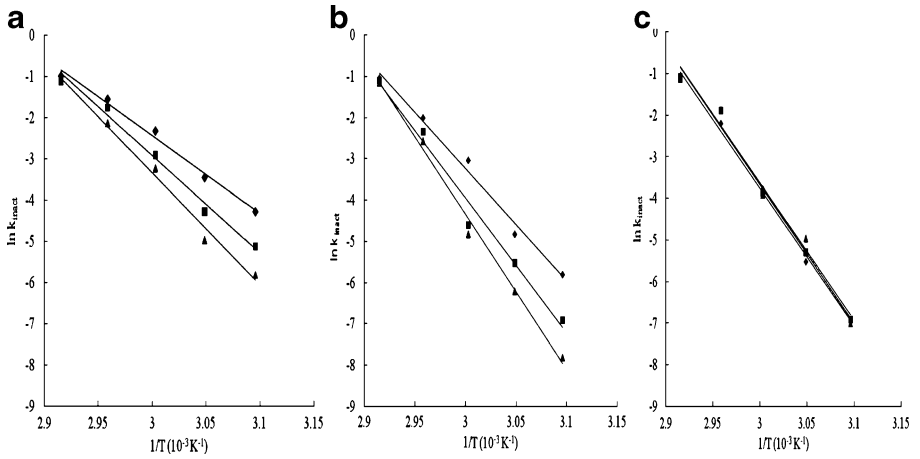

Fig. 7 Arrhenius plots of the denaturation rate constants of **a** wild-type, **b** A53S, and **c** H58I in 0 mM (*closed diamonds*), 2 mM (*closed squares*), and 5 mM (*closed triangles*) of $CaCl_2$ at different temperatures

In the case of wild-type enzyme and A53S mutant, the curves were sigmoid, and the midpoint of the mutant curve is decreased to almost 1.5 mM, reflecting that A53S binds more tightly to Ca^{2+}. From a structural point of view, Ser seemed more important for calcium binding than Ala because of its hydroxylic group (OH) in the side chain.

Unfolding Thermodynamic

Thermodynamic parameters for inactivation were evaluated for WT and two variants. Results showed the higher $\Delta G^{\#}$ values of unfolding for stable variants (Table 1). Mutants displayed a higher stability than wild type, indicating that the distance between the native state and the transition state has increased and, consequently, a larger input energy is required for their inactivation. In the absence of calcium, enzymes were more heat labile

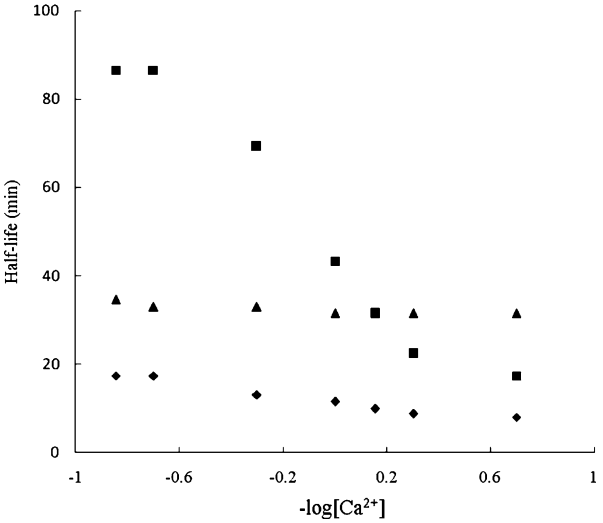

Fig. 8 Calcium ion titration of the rate of inactivation at 60 °C. Half-life of thermal inactivation of wild type (*closed diamonds*), A53S (*closed squares*), and H58I (*closed triangles*) is plotted as a function of the negative log $[Ca^{2+}]$. The reported half-lives are the average of two independent experiments, and the errors were ± 5%

because of lower energy barrier $\Delta G^{\#}$ of unfolding. It seems that the mutants displayed entropy-driven stabilization, and these kinds of reactions are spontaneous at high temperatures. Probably, Ca-dependent interactions or increased hydrophobic interactions appear to protect enzymes against thermal unfolding.

Conclusion

To date, no similar study involved cloning, sequencing, expression, and protein engineering has been carried on *B. megaterium* WHO α-amylase. Successful industrial use of amylases requires the ones that are highly thermostable and calcium independent. The elegant point of this research was to identify the stability-determining calcium-binding site and a stable BMW-amylase mutant in which the calcium dependency of stability is strongly reduced. This leads to the important conclusion that calcium binding is a useful but certainly not unique way to obtain stable protein.

Acknowledgement The authors express their gratitude to the research council of Tarbiat Modares University for the financial support during the course of this project.

References

1. Nielsen, J. E., & Borchert, T. V. (2000). *Biochimica et Biophysica Acta, 1543*, 253–274.
2. Tanaka, A., & Hoshino, E. (2002). *Biochemical Journal, 364*, 635–639.
3. Haki, G. D., & Rakshit, S. K. (2003). *Bioresource Technol, 89*, 17–34.
4. Tripathi, P., Hofmann, H., Kayastha, A. M., & Ulbrich-Hofmann, R. (2008). *Biophysical Chemistry, 137*, 95–99.
5. Vallee, B. L., Stein, E. A., Sumerwell, W. N., & Fischer, E. H. (1959). *Journal of Biological Chemistry, 234*, 2901–2905.
6. Imanaka, T., Shibazaki, M., & Takagi, M. (1986). *Nature, 324*, 695–697.
7. IIInase, A. (1999). *EJB, 2*, 7–15.
8. Yazdani, M., Naderi-Manesh, H., Khajeh, K., Soudi, M. R., Asghari, S. M., & Sharifzadeh, M. (2009). *Journal of Basic Microbiology, 49*, 119–127.
9. Tan, T. C., Mijts, B. N., Swaminathana, K., Patel, B. K. C., & Divne, C. (2008). *Journal of Molecular Biology, 378*, 850–868.
10. Tan, T. C., Yien, Y. Y., Patel, B. K. C., Mijts, B. N., & Swaminathana, K. (2003). *Acta Crystal, D59*, 2257–2258.
11. Sivakumar, N., Li, N., Tang, J. W., Patel, B. K. C., & Swaminathan, K. (2006). *FEBS Letters, 580*, 2646–2652.
12. Sambrook, J., & Russell, D. W. (2001). *Molecular cloning: a laboratory manual* (3rd ed.). New York: Cold Spring Harbor.
13. Owen, R. J., & Borman, P. (1987). *Nuclear Acids Research, 15*, 3631–3632.
14. Fisher, C. L., & Pei, G. K. (1997). *BioTechniques, 23*, 570–574.
15. Bradford, M. M. (1976). *Analytical Biochemistry, 72*, 248–254.
16. Laemmli, U. K. (1970). *Nature, 227*, 680–685.
17. Miller, G. L. (1959). *Analytical Chemistry, 31*, 426–428.
18. Arrhenius, S. (1889). *Zeitschrift fuÉr physikalische Chemie, 4*, 226–248.
19. http://www.expasy.ch/tools.
20. Fu, L. L., Xu, Z. R., Li, W. F., Shuai, J. B., Lu, P., & Hu, C. X. (2007). *Biotechnology Advances, 25*, 1–12.
21. Dong, G., Vieille, C., & Zeikus, J. G. (1997). *Applied and Environmental Microbiology, 63*, 3577–3584.
22. Janecek, S. (2002). *Biologia, 11*(57/Suppl), 29–41.
23. Danson, M. J., Hough, D. W., Russel, R. J., Tayler, G. L., & Pearl, L. (1996). *Protein Engineering, 9*, 629–630.

24. Lin, L. L., Huang, C. C., & Lo, H. F. (2008). *Process Biochemistry, 43*, 559–565.
25. D'Amico, S., Gerday, C., & Feller, G. (2003). *Journal of Molecular Biology, 332*, 981–988.
26. Violet, M., & Meunier, J. C. (1989). *Biochemical Journal, 263*, 665–670.
27. Hassan Sajedi, R., Naderi-Manesh, H., Khajeh, K., Ahmadvand, R., Ranjbar, B., Asoodeh, A., et al. (2005). *Enzyme and Microbial Technology, 36*, 666–671.
28. Takasaki, Y. (1982). *Agricultural and Biological Chemistry, 46*, 1539–1547.
29. Kanno, M. (1986). *Agricultural and Biological Chemistry, 50*, 23–31.
30. Tsvetkov, V. T., & Emanuilova, E. I. (1989). *Applied Microbiology and Biotechnology, 31*, 246–248.
31. Hagihara, H., Igarashi, K., Hayashi, Y., Kitayama, K., Endo, K., Ozawa, T., et al. (2002). *J Appl Glycosci, 49*, 281–289.